

# Computational and NMR Studies on the Complexation of Lithium Ion to 8-Crown-4

Alex van der Ham<sup>+, [a]</sup>, Thomas Hansen<sup>+, [a, b]</sup>, Gerrit Lodder,<sup>[a]</sup> Jeroen D. C. Codée,<sup>[a]</sup> Trevor A. Hamlin,<sup>[b]</sup> and Dmitri V. Filippov<sup>\*[a]</sup>

Lithium ion selective crown ethers have been the subject of much research for a multitude of applications. Current research is aimed at structurally rigidifying crown ethers, as restructuring of the crown ether ring upon ion binding is energetically unfavorable. In this work, the lithium ion binding ability of the relatively rigid 8-crown-4 was investigated both computationally by density functional theory calculations and experimentally by <sup>1</sup>H and <sup>7</sup>Li NMR spectroscopy. Although both computational and experimental results showed 8-crown-4 to bind lithium ion, this binding was found to be weak compared to

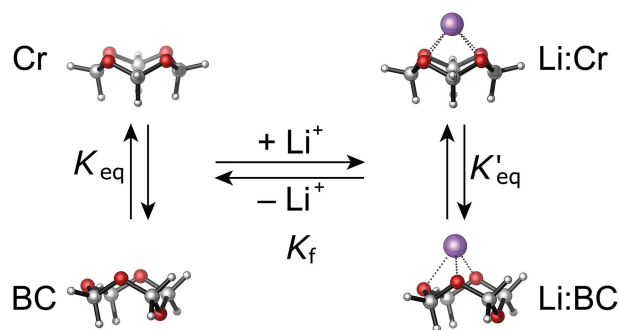
larger crown ethers. The computational analysis revealed that the complexation is driven by enthalpy rather than entropy, illustrating that rigidity is only of nominal importance. To elucidate the origin of the favorable interaction of lithium ion with crown ethers, activation strain analyses and energy decomposition analyses were performed pointing to the favorable interaction being mainly electrostatic in nature. 8-crown-4 presents the smallest crown ether reported to date capable of binding lithium ion, possessing two distinct conformations from which it is able to do so.

## 1. Introduction

Crown ethers are well-known for their ability to selectively bind metal cations. Lithium ion selective crown ethers in particular find application in a wide variety of fields including solid-state electrolytes,<sup>[1]</sup> membrane electrodes,<sup>[2]</sup> isotopic enrichment,<sup>[3]</sup> and the recovery of lithium from aqueous solutions.<sup>[4]</sup>

Although the most significant factors that determine the binding of a crown ether to a particular metal cation are somehow related to the ring size, making accurate predictions about the binding strength is not entirely straightforward.<sup>[5]</sup> Already early on, large crown ethers were found to be highly flexible, requiring an increase of entropic cost in reorganizing the molecule to permit ion complexation. This reorganization concomitantly introduces a significant ring strain, which adds a further energy cost due to increased enthalpy upon ion binding.<sup>[6]</sup> Therefore, several studies have looked into the effect of rigidifying crown ethers, for example computational studies wherein crown ethers were embedded in graphene or in graphene-like model compounds.<sup>[6b,7]</sup>

In this regard, it is surprising that the complexation of lithium ion with the small and relatively rigid crown ether, 8-crown-4 (8C4), has thus far received virtually no attention. Also known as tetroxocane, 8C4 was first synthesized by Staudinger and Lüthy in 1925 via the thermal cracking of acetylated paraformaldehyde.<sup>[8]</sup> The ability of 8C4 to bind lithium ions was to the best of our knowledge suggested in 1991. Using Hartree-Fock calculations with the minimal STO-3G basis set, Fujimoto and co-workers<sup>[9]</sup> demonstrated a favorable 160 kcal·mol<sup>-1</sup> energy difference upon complexation of lithium ion to the crown conformation of 8C4, forming a so-called “perching complex”.<sup>[10]</sup> Although eight-membered rings can adopt a variety of conformations,<sup>[11]</sup> NMR studies show that 8C4 only exists in a crown (Cr) or boat-chair (BC) conformation in solution (Scheme 1).<sup>[12]</sup> We hypothesized that because 8C4 already exists in a stable conformation from which it can bind lithium ion, it would not suffer an additional energy cost upon complexation.



**Scheme 1.** Equilibria for the BC⇌Cr interconversion of 8C4 and their respective lithium ion complexes. Note that the complexation constant  $K_f$  is the average for lithium ion binding to both the BC and Cr conformation of 8C4.  $K_{eq}$  and  $K'_{eq}$  are the equilibrium constants for the BC⇌Cr and Li:BC⇌Li:Cr interconversion, respectively. Bistriflimide counter ions are omitted from the scheme for clarity.

[a] A. van der Ham,<sup>+</sup> T. Hansen,<sup>+</sup> Dr. G. Lodder, Dr. J. D. C. Codée, Dr. D. V. Filippov  
Leiden Institute of Chemistry, Leiden University, Einsteinweg 55, 2333 CC Leiden (The Netherlands)  
E-mail: filippov@chem.leidenuniv.nl

[b] T. Hansen,<sup>+</sup> Dr. T. A. Hamlin  
Department of Theoretical Chemistry, Amsterdam Center for Multiscale Modeling (ACMM), Vrije Universiteit Amsterdam, De Boelelaan 1083, 1081 HV Amsterdam (The Netherlands)

[\*] These authors contributed equally to this work

Supporting information for this article is available on the WWW under <https://doi.org/10.1002/cphc.201900496>

© 2019 The Authors. Published by Wiley-VCH Verlag GmbH & Co. KGaA. This is an open access article under the terms of the Creative Commons Attribution Non-Commercial NoDerivs License, which permits use and distribution in any medium, provided the original work is properly cited, the use is non-commercial and no modifications or adaptations are made.

In other words, 8C4 may well complex cations better than expected on the basis of its ring size.

In the present study, DFT calculations were performed in order to determine the binding strength and nature of 8C4 with  $\text{Li}^+$  in nitromethane. To experimentally corroborate the findings,  $^1\text{H}$ -NMR and  $^7\text{Li}$ -NMR experiments were conducted at different temperatures to ascertain the occurrence of  $\text{Li}^+$  ion binding and to determine the equilibrium constants ( $K_{\text{eq}}$  and  $K'_{\text{eq}}$ ) for  $\text{BCr} \rightleftharpoons \text{Cr}$  and  $\text{Li:BCr} \rightleftharpoons \text{Li:Cr}$  interconversion at these temperatures. In addition,  $^7\text{Li}$  NMR experiments were performed to determine the complexation constant  $K_f$ , as a measure for the binding strength of lithium ion to 8C4 (Scheme 1).

## Experimental Section

### General Methods

Lithium bistriflimide (99.95 % trace metal basis) from Sigma-Aldrich and nitromethane- $d_3$  with 1 % TMS from Acros Organics were used without further purification. Commercial nitroethane was purified according to the method described for nitromethane.<sup>[13]</sup> In short, a 100 mL portion of nitroethane was sequentially washed with equal volumes of saturated  $\text{NaHCO}_3$ ,  $\text{NaHSO}_3$ , water, 5 %  $\text{H}_2\text{SO}_4$ , water and dilute  $\text{NaHCO}_3$ . Subsequently, it was dried for several hours over Drierite® prior to being distilled at atmospheric pressure. The clear, colorless solvent was stored over 4 Å molecular sieves in brown bottles at 4 °C until use.

### Synthesis

8-crown-4: 1,3,5,7-tetraoxacyclooctane was synthesized using a modified literature procedure.<sup>[12]</sup> Paraformaldehyde (5 g) was added as a suspension in water (5 mL) to 250 mL of 1,1,2,2-tetrachloroethane, and the mixture was vigorously stirred and heated to 100 °C. Next, 2-aminonaphthalene-5-sulfonic acid (200 mg) was added and the mixture stirred for another 2 hours. The mixture was allowed to cool to room temperature and the tetrachloroethane separated from the clear red aqueous phase. The organic phase was dried over  $\text{K}_2\text{SO}_4$ , filtered and evaporated under reduced pressure (25 mbar). The majority of solvent was removed at 60 °C whereas the final 10 mL was carefully removed at room temperature, leaving behind approximately 1 mL of a dark orange solution from which colorless crystals deposited overnight at -20 °C. The solvent was separated, the crystals carefully washed with pentane (2 × 5 mL), dried under vacuum at room temperature and further purified by vacuum sublimation. The crude crystalline material (60 mg) was charged in a vacuum flask fitted with a water cooled cold finger. The flask was put under vacuum and slowly heated on an oil bath. White needles started to deposit on the cold finger at 80 °C. The temperature was slowly raised further to 120 °C and kept at this temperature for 30 min, at which point no further material deposited. The final yield of crown ether was 50 mg in the form of pure white crystals. The crystals were stored in the dark at -20 °C until use.  $^1\text{H}$  NMR (500 MHz,  $\text{CDCl}_3$ )  $\delta$  5.04 (brs);  $^{13}\text{C}$  NMR (125 MHz,  $\text{CDCl}_3$ )  $\delta$  95.7 (brs); HRMS (ESI-TOF)  $m/z$ :  $[\text{M} + \text{Na}]^+$  calcd for  $\text{C}_4\text{H}_8\text{O}_4\text{Na}$  143.03203 found 143.03167,  $[\text{M} + \text{K}]^+$  calcd for  $\text{C}_4\text{H}_8\text{O}_4\text{K}$  159.00597, found 159.00562.

### NMR Experiments

NMR experiments were performed on a Bruker AV500 NMR instrument equipped with a BBFO probe head for 5 mm outer diameter

tubes. Spectra were recorded at 500 MHz for  $^1\text{H}$ , 125 MHz for  $^{13}\text{C}$  and 194 MHz for  $^7\text{Li}$ . Experiments performed in non-deuterated solvent used external locking with a coaxial acetone- $d_6$  insert, and  $^1\text{H}$  spectra referenced from the residual solvent signal set at 2.05 ppm. In the  $^1\text{H}$  spectra selective suppression of the nitroethane quartet was applied. For the  $^7\text{Li}$  experiments, spectra were referenced from 9.7 M LiCl in  $\text{D}_2\text{O}$ . The chemical shift of  $\text{LiNTf}_2$  at the same concentration in the same solvent in the absence of crown ether was used to compensate for any concentration dependent effects. The chemical shift data was analyzed using MatLab. A detailed description of the data analysis is given in the Supplementary Information.

### Computational Methods

Crown ethers were initially optimized by a conformer distribution search included in the Spartan 10 program.<sup>[14]</sup> The conformer distribution was computed in the gas phase at the DFT level of theory using B3LYP as hybrid functional and 6-31G(d) as basis set. For the lithium:crown ether complexes, lithium ions were initially positioned at a fixed distance of 2 Å from two opposing oxygen atoms in the Spartan 10 software. After an initial energy minimization this distance restriction was removed and the structure again optimized. The resulting structure library was further refined using the Gaussian 09 Rev. D.01<sup>[15]</sup> with the use of the M06-2X hybrid functional<sup>[16]</sup> and 6-311+G(d,p) basis set. Geometries were optimized in the gas-phase and subsequently re-optimized in combination with the SMD model to include solvent effects, using nitromethane as the solvent parameter.<sup>[17]</sup> The denoted free Gibbs energy was calculated using Equation (1), in which  $\Delta E_{\text{gas}}$  is the gas-phase energy (electronic energy),  $\Delta G_{\text{gas,QH}}^T$  ( $T = 293.15 \text{ K}$ ,  $p = 1 \text{ atm.}$ ,  $C = 1 \text{ M}$ ) is the sum of corrections from the electronic energy to the free Gibbs energy in the quasi-harmonic oscillator approximation, including zero-point-vibrational energy, and  $\Delta G_{\text{solv}}$  is their corresponding free solvation Gibbs energy [Eq. (1)]. The  $\Delta G_{\text{gas,QH}}^T$  were computed using the quasi-harmonic approximation in the gas phase according to the work of Truhlar - the quasi-harmonic approximation is the same as the harmonic oscillator approximation except that vibrational frequencies lower than  $100 \text{ cm}^{-1}$  were raised to  $100 \text{ cm}^{-1}$  as a way to correct for the breakdown of the harmonic oscillator model for the free energies of low-frequency vibrational modes.<sup>[18]</sup> All stationary points found were checked for either no imaginary frequencies for local minima or one imaginary frequency for transition state structures.

$$\Delta G_{\text{nitromethane}}^T = \Delta E_{\text{gas}} + \Delta G_{\text{gas,QH}}^T + \Delta G_{\text{solv}} \quad (1)$$

For relevant optimized structures the spin-spin coupling constants were calculated according to the work of Rablen and Bally with the use of 6-311G(d,p) u + 1 s as basis set and SMD( $\text{CH}_3\text{NO}_2$ ) as solvent model.<sup>[19]</sup> The calculated total nuclear spin-spin coupling terms were used as calculated spin-spin coupling constants. The isotropic magnetic shielding tensors were computed using the gauge-independent atomic orbital (GIAO) methodology and the isotropic magnetic shielding tensors were averaged over all symmetry related carbons and hydrogens where applicable.  $^1\text{H}$  chemical shifts were calculated with the use of B3LYP/aug-cc-pVDZ. Activation strain analyses using Equation (2) and energy decomposition analyses using Equation (3) were performed using ADF 2017.103<sup>[20]</sup> in the gas phase at M06-2X/TZ2P on the geometries optimized at SMD( $\text{CH}_3\text{NO}_2$ )-M06-2X/6-311+G(d,p) in Gaussian 09. Molecular structures were illustrated using CYLview.<sup>[21]</sup>

$$\Delta E = \Delta E_{\text{strain}} + \Delta E_{\text{int}} \quad (2)$$

**Table 1.** Computed geometries of the two conformers of 8C4, their respective complexes with lithium ion and their corresponding solution-phase Gibbs free energy, gas-phase Gibbs free energy, enthalpy, entropy contribution and solvation energy in nitromethane all in kcal mol<sup>-1</sup>. Energies are calculated at SMD(CH<sub>3</sub>NO<sub>2</sub>)-M06-2X/6-311+G(d,p) at *T* = 293.15 K and are reported relative to the values computed for the unbound Cr conformer. For the complexed crown ethers the distances between the lithium ion and ring oxygens are given in Å. The out-of-the-plane bending angle between the Li–O bond and the C–O–C plane ( $\phi$ ) is defined according to Cui *et al.*<sup>[26]</sup> and averaged over all oxygen atoms bound to the lithium ion.

	Li 8C4 (Cr)	Li 8C4 (BC)	Li:8C4 (Cr)	Li:8C4 (BC)
$\phi$ -angle [°]				
$\Delta\Delta G_{\text{MeNO}_2}$	0.0	0.8	–13.7	–14.6
$\Delta\Delta G_{\text{gas}}$	0.0	–1.6	–50.2	–51.0
$\Delta\Delta H_{\text{gas}}$	0.0	–0.8	–59.3	–59.0
$T\Delta\Delta S_{\text{gas}}$	0.0	0.8	–9.1	–8.0
$\Delta\Delta G_{\text{solvation}}$	0.0	2.4	36.5	36.4

$$\Delta E_{\text{int}} = \Delta E_{\text{elstat}} + \Delta E_{\text{Pauli}} + \Delta E_{\text{oi}} \quad (3)$$

## 2. Results and Discussion

### 2.1. DFT Calculations

The monocyclic 8C4 yields two well-defined energy minima in which it binds the guest (Scheme 1, Table 1). The 8C4 spontaneously binds a lithium ion in both the Cr and BC conformations, as shown by the lower free energy of the complexes (Li:8C4) compared to their separated species (Li<sup>+</sup> + 8C4) (Table 1). The BC conformer of 8C4 is intrinsically more stable than the Cr conformer (1.6 kcal mol<sup>-1</sup>, Table 1) in terms of free energy, both enthalpically due to less transannular strain and due to a more stabilizing entropy term.<sup>[22]</sup> Electron diffraction data on 8C4 in the gas phase agreeingly shows a [Cr]:[BC] ratio of 1:2.1 at 100 °C indicating the higher thermodynamic stability of the BC conformer in the absence of solvation effects.<sup>[23]</sup> In the polar solvent nitromethane, however, the Cr conformer, with its higher dipole moment,<sup>[24]</sup> is more stable than the BC due to a 2.4 kcal mol<sup>-1</sup> difference in solvation energy (Table 1). Overall, therefore, in its uncoordinated form, the Cr conformer in nitromethane is 0.8 kcal mol<sup>-1</sup> lower in energy than the BC conformer. This computational analysis agrees with experimental data on the effect of the medium on the [Cr]:[BC] distribution whereby the Cr is preponderant in polar solvents.<sup>[12,24]</sup> The energy barrier for the interconversion between the Cr and BC conformer was found to be 13.4 kcal mol<sup>-1</sup> (Table S10). In the solid state 8C4 exists exclusively in the Cr conformation.<sup>[25]</sup>

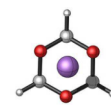
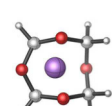
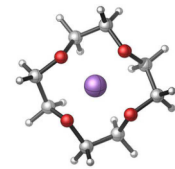
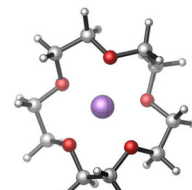
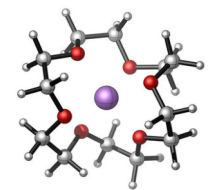
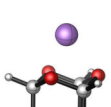
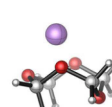
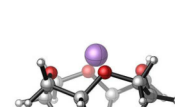
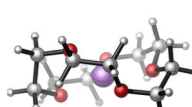
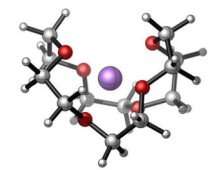
Complexation of a lithium ion with the Cr conformer in nitromethane is exergonic by 13.7 kcal mol<sup>-1</sup>, whereas that of the BC conformer is slightly more exergonic by 14.6 kcal mol<sup>-1</sup> (Table 1). The energy barrier for interconversion of the bound crown ether (12.2 kcal mol<sup>-1</sup>) is nearly the same as that of the unbound crown (Table S10). The BC conformer only coordinates the lithium ion with three of the ring oxygens, whereas the Cr conformer binds with all four oxygens. Since in both the crown

(Li:Cr) and boat-chair (Li:BC) complex the average Li...O distance was found to be 2.107 Å the additional Li...O bond in the Li:Cr complex should result in a stronger enthalpic binding for Cr to lithium ion compared to BC. The nearly equal binding enthalpies of the Li:BC and the Li:Cr complexes are therefore unexpected. However, a closer inspection of the geometry of the complexes revealed a much larger average out-of-the-plane bending angle ( $\phi$ ) between the Li...O bond and the C–O–C plane in the Li:Cr complex (85° versus 67°). As demonstrated by Cui *et al.*, larger  $\phi$ -angles in crown complexes significantly diminish the stabilizing ion-dipole interaction and hence the strength of host-guest binding.<sup>[24]</sup> Thus, trioxane (6C3), which also binds lithium ion with three Li...O bonds of 2.1 Å, has an almost two-fold weaker binding affinity than 8C4 (7.7 kcal mol<sup>-1</sup>, Table 2) due to its  $\phi$ -angle of approximately 90°.<sup>[27]</sup>

Interestingly, the commercially available tetramethyl-8C4 (metaldehyde) binds lithium ions more strongly than 8C4 itself (binding solution-phase Gibbs free energy of 20.0 kcal mol<sup>-1</sup>) as indicated by DFT calculations (SI Structures S11 and S12), yet its insolubility in all tested solvents precluded experimental verification.

For comparison, the binding free energy of lithium ion was calculated not only for the smaller crown ether 6C3 but also for the larger crown ethers 12C4, 15C5 and 18C6 (Table 2). The data shows that, with increasing ring size, there is a small rise in entropic loss upon complexation of lithium ion, whereas the binding enthalpy increases significantly with accompanying decrease of the  $\phi$ -angle. Thus, for 8C4 and 6C3, the comparatively small binding enthalpy is to some extent compensated by the smaller loss of entropy upon lithium ion binding, but by far not enough to make the binding of these small crowns to lithium ion similar in strength to that found for the larger crown ethers. The large differences in binding enthalpy reflect the fact that, whereas with the larger crown ethers (12C4, 15C6 and 18C6) the lithium ion is located within the ring in a nesting complex, the ion sits on top of 8C4 due to the small cavity size; i.e. forms two perching complexes Li:BC and Li:Cr.<sup>[10]</sup> Regarding our hypothesis, 8C4 indeed benefits in terms of entropic cost

**Table 2.** Computed geometries and the relative corresponding solution-phase Gibbs free energy, gas-phase Gibbs free energy, enthalpy, entropy contribution and solvation energy in nitromethane all in  $\text{kcal mol}^{-1}$  for the lithium complexes of 6C3, 8C4, 12C4, 15C5 and 18C6 relative to their separated species. All energies are as calculated at SMD(CH<sub>3</sub>NO<sub>2</sub>)-M06-2X/6-311 + G(d,p) at  $T=293.15$  K. The room temperature  $K_f$  values for the literature crown ethers were obtained in MeNO<sub>2</sub>, whereas that for 8C4 was in EtNO<sub>2</sub> at room temperature. The out-of-the-plane bending angle between the Li...O bond and the C–O–C plane ( $\phi$ ) is defined according to Cui *et al.*<sup>[26]</sup> and averaged over all oxygen atoms bound to the lithium ion. N.B. = no binding.

	Li:6C3	Li:8C4	Li:12C4	Li:15C5	Li:18C6
					
					
$\phi$ -angle [°]	89.6	66.6	54.0	50.1	46.9
$\Delta G_{\text{MeNO}_2}$	-7.7	-14.6	-40.0	-46.3	-46.8
$\Delta H_{\text{gas}}$	-43.5	-59.0	-93.5	-107.6	-117.4
$T\Delta S_{\text{gas}}$	-7.4	-8.0	-9.3	-10.1	-11.4
$\Delta G_{\text{solvation}}$	28.4	36.4	44.2	51.2	59.2
experimental $\log(K_f)$	N.B. <sup>[30]</sup>	$1.71 \pm 0.46$	$3.65 \pm 0.04$ <sup>[31]</sup> > 4 <sup>[32]</sup>	> 5 <sup>[31]</sup> > 4 <sup>[32]</sup>	> 5 <sup>[31]</sup> > 4 <sup>[32]</sup>

by not having to undergo significant restructuring, yet this effect is only marginal.

To further understand the nature and strength of the interaction between the Li<sup>+</sup> and the crown ethers the activation strain model (ASM) was used.<sup>[28]</sup> This method decomposes the electronic energy ( $\Delta E$ ) in two terms, the strain energy ( $\Delta E_{\text{strain}}$ ) arising from the structural reorganization of the crown ether associated with the accommodation of the Li<sup>+</sup> and the interaction energy ( $\Delta E_{\text{int}}$ ) originating from the interaction between the Li<sup>+</sup> and crown ether. The interaction energy was further analyzed by applying a canonical energy decomposition analysis (EDA).<sup>[29]</sup> The  $\Delta E_{\text{int}}$  is decomposed into three terms: Pauli repulsive orbital interactions ( $\Delta E_{\text{Pauli}}$ ) between closed-shell orbitals, classical electrostatic interaction ( $\Delta V_{\text{elstat}}$ ) and stabilizing orbital interactions ( $\Delta E_{\text{oi}}$ ) that account for charge transfer and polarization.

Table 3 summarizes the results of the ASM and EDA analyses of the Li<sup>+</sup> crown ether complexes. It can be seen that the trends in electronic energy are mainly determined by the  $\Delta E_{\text{int}}$  as differences in the  $\Delta E_{\text{strain}}$  are much smaller. Increasing

**Table 3.** Energy decomposition analysis terms (in  $\text{kcal mol}^{-1}$ ) computed on the lithium crown ether complexes at M06-2X/TZ2P//SMD(CH<sub>3</sub>NO<sub>2</sub>)-M06-2X/6-311 + G(d,p).

	Li:6C3	Li:8C4 (BC)	Li:8C4 (Cr)	Li:12C4	Li:15C5	Li:18C6
$\Delta E$	-44.1	-59.2	-59.4	-93.4	-105.2	-114.8
$\Delta E_{\text{strain}}$	2.9	1.7	4.6	9.9	15.5	18.7
$\Delta E_{\text{int}}$	-47.0	-60.9	-64.0	-103.3	-120.7	-133.5
$\Delta E_{\text{Pauli}}$	11.0	16.5	14.4	24.2	22.7	23.8
$\Delta V_{\text{elstat}}$	-33.5	-46.9	-46.9	-82.5	-94.4	-103.5
$\Delta E_{\text{oi}}$	-24.5	-30.6	-31.5	-45.0	-49.0	-53.7

the size of the crown ether results in a much more stabilizing  $\Delta E_{\text{int}}$  and a slightly more destabilizing  $\Delta E_{\text{strain}}$  originating from the required reorganization of the crown ether. As hypothesized, 8C4 has the least amount of destabilizing  $\Delta E_{\text{strain}}$  as it requires only a negligible amount of reorganization to bind Li<sup>+</sup>, even less than the smaller 6C3. The energy decomposition further reveals that the interaction is mainly electrostatic in nature, originating from the stabilizing interaction between the Li<sup>+</sup> and the  $\delta^-$  oxygen atoms of the crown ether. Besides the electrostatic interaction, in all systems there are key donor-acceptor orbital interactions between the lone pair  $\pi$ -type molecular orbitals of the oxygen atoms of the crown ether and the unoccupied s- and 2p-type AOs of the Li<sup>+</sup>.<sup>[34]</sup>  $\Delta E_{\text{Pauli}}$  only marginally counteracts the stabilizing  $\Delta E_{\text{oi}}$  and  $\Delta V_{\text{elstat}}$  interactions.

## 2.2. NMR Experiments

To experimentally corroborate the computational findings, variable temperature NMR experiments were conducted to determine the equilibrium constants ( $K_{\text{eq}}$  and  $K'_{\text{eq}}$ ) for the BC $\rightleftharpoons$ Cr and Li:BC $\rightleftharpoons$ Li:Cr interconversion. In order to accurately investigate the interaction of lithium ion with 8C4, interfering interactions, such as desolvation and ion pair dissociation, had to be reduced to a minimum, as these would introduce an additional energy cost to lithium ion complexation by the crown ether. Therefore, nitroalkanes were selected as solvents for the NMR experiments as these benefit from a low Gutmann Donor Number (2.7 and 5.0  $\text{kcal mol}^{-1}$  for CH<sub>3</sub>NO<sub>2</sub> and EtNO<sub>2</sub>, respectively<sup>[35]</sup>), which is a measure for the ability of solvents to

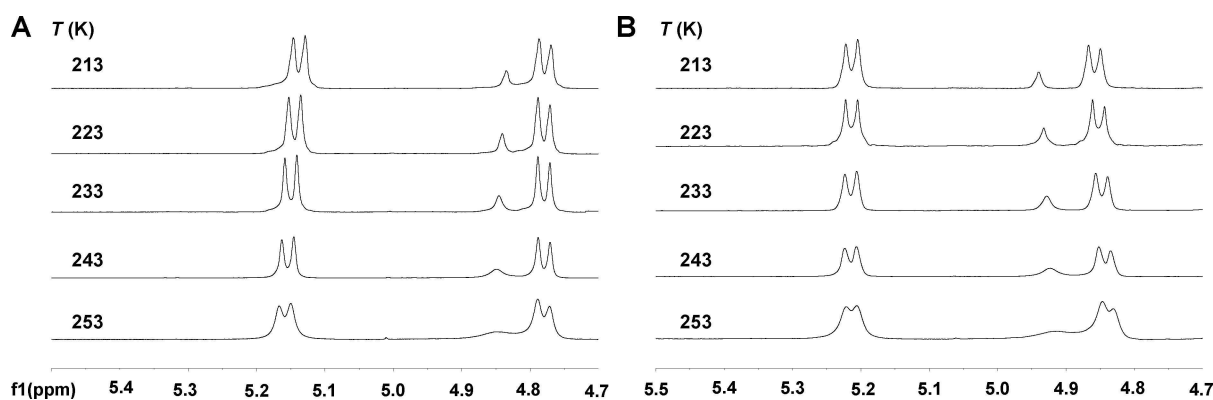


**Figure 1.** Variable temperature  $^1\text{H}$  spectra of 8C4 in nitroethane in the absence (A) and presence (B) of a stoichiometric amount of LiNTf<sub>2</sub>. At  $-20^\circ\text{C}$ , the splitting of the crown conformer signals becomes apparent. Note the overall downfield shift in the presence of lithium salt.

donate electron density to a solute. Moreover the high permittivity of nitroalkanes results in only minimal ion pair formation.<sup>[36]</sup> In addition, the low melting point of nitroethane made it suitable for low temperature NMR experiments. Lithium bistriflimide (LiNTf<sub>2</sub>) was used as the lithium source because of its high dissociation constant,<sup>[37]</sup> resulting in little ion pairing and concomitant high solubility in nitroalkanes,<sup>[38]</sup> again, permitting low temperature NMR experiments. Based on previous findings, the influence of the anion was deemed to be insignificant.<sup>[39]</sup>

To synthesize 8C4, a reported procedure with modified work-up and purification protocol was employed that relies on the acid catalyzed hydrolysis of paraformaldehyde in a water-tetrachloroethane mixture at elevated temperature.<sup>[12]</sup> Thus, upon completion of the reaction the organic layer was not evaporated to dryness, but rather concentrated to a small volume and the product allowed to crystallize overnight at low temperature. Next, the crystals were washed with a small amount of pentane and subjected to vacuum sublimation to give 50 mg of pure 8C4, starting from 5 g of paraformaldehyde. The sample of 8C4 thus obtained was used in the NMR experiments described further.

Figure 1 shows the proton spectra of 8C4 in nitroethane at various temperatures in the absence (A) and presence (B) of lithium ion, which was introduced by the addition of LiNTf<sub>2</sub> to the nitroethane solution of 8C4. At room temperature both in the absence and presence of lithium ion only a broad singlet at around 5.0 ppm is observed indicating a fast interconversion of the conformers on the NMR time-scale. Upon cooling, the two characteristic doublets of the crown conformer become apparent and a discernible singlet of the boat-chair conformer appears at  $-20^\circ\text{C}$ . To unambiguously assign the signals, NMR spectra of the free crown ethers were computed. This confirmed that the downfield doublet corresponds to the annular protons and the upfield doublet to the transannular protons, as can be expected on the basis of normal anisotropic effects in heterocyclic ring systems.<sup>[40]</sup> A comparison between the observed and calculated chemical shifts is given in the Supporting Information (Figure S4).

At  $-20^\circ\text{C}$  in nitroethane, 8C4 exists predominantly in the crown conformation with a [Cr]:[BC] ratio of 10:1, which increases upon cooling down to a value of 50:1 at  $-60^\circ\text{C}$  (Table S1 and S2 Supporting Information). The observed conformer distributions and their temperature dependencies are in qualitative agreement with the ones reported for 8C4 in different solvents.<sup>[12,22,41]</sup> When the values are extrapolated to room temperature a [Cr]:[BC] ratio of 3:1 is found (Table 4,

**Table 4.** Dipole moments ( $D$ ) in Debye, equilibrium constants  $K_{\text{eq}}$ , and the associated change in enthalpy and the entropy contribution ( $T\Delta S$ ) in kcal mol<sup>-1</sup> for the BC $\rightleftharpoons$ Cr and Li:BC $\rightleftharpoons$ Li:Cr interconversion of 8C4 in different solvents.

Entry	System	$D$	$K_{\text{eq}}$ ( $T=293\text{ K}$ )	$\Delta H$	$T\Delta S$	Ref.
1	EtNO <sub>2</sub> (+ 1 eq. LiNTf <sub>2</sub> )	–	5.60	–1.97	–0.97	This work
2	EtNO <sub>2</sub>	3.61	3.04	–4.28	–3.64	This work
3	CD <sub>3</sub> CN	3.92	2.67	–2.74	–2.17	[12]
4	CDCl <sub>3</sub>	1.08	0.81	–2.13	–2.26	[12]
5	CHCl <sub>2</sub> F	1.29	1.04	–1.78	–1.76	[41]

Entry 2), which is in excellent agreement with the computed solution-phase Gibbs free energy difference of 0.8 kcal mol<sup>-1</sup> which corresponds to a [Cr]:[BC] ratio of 4:1.

When a stoichiometric amount of lithium salt is added Li:8C4 complexes are formed. Indications for this are an overall downfield shift of all the resonances in the  $^1\text{H}$ -NMR spectrum upon the addition of the lithium salt (Figure 1), as well as a downfield field of the spectral line in the  $^7\text{Li}$ -NMR spectrum when the temperature was lowered from 263 K to 203 K, as a result of tighter binding of lithium ion to the crown ether (Figure S3).<sup>[42]</sup> At  $-60^\circ\text{C}$  a [Li:Cr]:[Li:BC] ratio of 20:1 is observed which goes to a ratio of 9:1 at  $-20^\circ\text{C}$ , and finally yields an extrapolated value of 5.6:1 at room temperature that corresponds to a free energy difference of  $-1.5$  kcal/mol (Table 4, Entry 1). The computed value of the free energy for Li:BC $\rightleftharpoons$ Li:Cr interconversion of 0.9 kcal mol is within the computa-

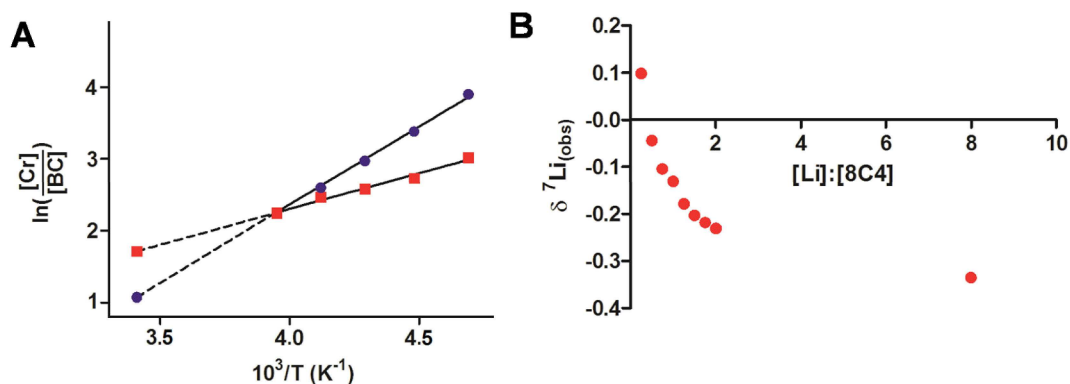


**Figure 2.** A) Van't Hoff plots for the  $\text{BC} \rightleftharpoons \text{Cr}$  and  $\text{Li}:\text{BC} \rightleftharpoons \text{Li}:\text{Cr}$  interconversion in the absence (●) and presence (■) of a stoichiometric amount of lithium salt in nitroethane. B) Observed <sup>7</sup>Li chemical shift plotted against  $[\text{Li}^+]:[\text{8C4}]$  ratio at room temperature. <sup>7</sup>Li-NMR measurements were performed in  $\text{MeNO}_2\text{-}d_3$ . Note the downfield shift with increasing amounts of 8C4.

tional error, taking into account the reported accuracy of SMD solvation model for charged species.<sup>[17]</sup>

Next, the experimental values of the enthalpy ( $\Delta H$ ) and the entropy contribution ( $T\Delta S$ ) for the  $\text{BC} \rightleftharpoons \text{Cr}$  and  $\text{Li}:\text{BC} \rightleftharpoons \text{Li}:\text{Cr}$  equilibrium were determined from the NMR data shown in Figure 1 using van't Hoff plots. The relative populations of the 8C4 conformers, both free and bound to Li ion, are plotted against the inverse absolute temperature (Figure 2A, Table 4). The slopes and intercepts of these plots yield the enthalpy and entropy contributions to the free energy change that drives the conformational interconversion. The increasing abundance of BC at higher temperatures, both observed (Table S1) and predicted by the DFT calculations, is due to an increase in entropy in the interconversion of Cr into BC ( $0.8 \text{ kcal mol}^{-1}$ , Table 1). It is seen that upon addition of lithium ions, the Li ion bound BC conformer of 8-crown-4 becomes somewhat pre-organized, resulting in a less negative entropy term ( $T\Delta S$ ) for the  $\text{Li}:\text{BC} \rightleftharpoons \text{Li}:\text{Cr}$  equilibrium.

Finally, the complexation constant of  $\text{Li}^+$  ion to 8C4 was determined by measuring the <sup>7</sup>Li chemical shift in nitromethane at different  $[\text{Li}^+]:[\text{8C4}]$  ratios at room temperature (Figure 2B). From the equation developed by Roach (see page 5 of Supporting Information for the derivation), a complexation constant  $\log K_f$  of  $1.71 \pm 0.46$  could be found for the 1:1 complex. When the same data was fitted with the BindFit software, a similar value of  $\log K_f$  of  $2.09 \pm 0.09$  was obtained.<sup>[43]</sup> These values are indeed small compared to the  $K_f$  values of the larger crown ethers (Table 2). Thus, the comparatively weak interaction of lithium ion with 8C4 as experimentally observed is in line with the calculated value of the solution-phase Gibbs free energy of binding (Table 2). Although 1:2 complexes of 8C4 with  $\text{Li}^+$  were computed to be favorable (Table S8), they were not observed experimentally.<sup>[44]</sup>

### 3. Conclusions

In the present study the lithium ion binding ability of 8C4 was investigated both computationally and experimentally, to verify

whether its intrinsic rigidity would facilitate in ion binding. DFT computations showed 8C4 to exist in two stable conformers, the crown (Cr) and boat-chair (BC), which in their unbound state differ by  $0.8 \text{ kcal mol}^{-1}$  in favour of the Cr conformer. Upon binding to lithium ion both conformers showed the formation of stable perching complexes, evidenced by a decrease in Gibbs free energy, with a slight preference for the  $\text{Li}:\text{BC}$  complex of  $0.9 \text{ kcal mol}^{-1}$ .

Experimentally, the formation of Li complexes with 8C4 was supported by the observance of a downfield shift of all resonances in the <sup>1</sup>H NMR experiments, as well as the downfield shift of the <sup>7</sup>Li resonance.

By means of <sup>7</sup>Li NMR a binding constant for 8C4 of  $\log K_f = 1.71 \pm 0.46$  was found, which is weaker compared to that found previously for larger crown ethers. In fact, this value continues the known trend that larger rings give better binding. The poor binding ability of 8C4 was attributed to an unfavourably large binding angle, and the fact that although there is indeed a smaller entropic loss upon ion binding compared to larger crown ethers, this effect is only marginal in compensating the significantly less favourable binding enthalpy.

The nature of lithium ion:crown ether binding was further studied using the activation strain model. This demonstrated that indeed 8C4 has a better pre-organized structure from which it can bind, yet binding is by and large driven by the interaction energy. A further energy decomposition analysis revealed the electrostatic contribution to the interaction energy to be paramount in ion binding. To conclude, 8-crown-4 presents the smallest crown ether reported to date capable of binding lithium ion, possessing two distinct conformations from which it is able to do so.

### Acknowledgements

The authors thank the SURFsara for use of the Lisa supercomputer and kindly acknowledge Mark Somers for technical support.

## Conflict of Interest

The authors declare no conflict of interest.

**Keywords:** activation strain model · density functional calculations · crown ethers · lithium ion binding · perching complex

- [1] M. Gao, Y. Wang, Q. Yi, Y. Su, P. Sun, X. Wang, J. Zhao, G. Zou, *J. Mater. Chem. A* **2015**, *3*, 20541–20546.
- [2] K. Kimura, H. Oishi, T. Miura, T. Shono, *Anal. Chem.* **1987**, *59*, 2331–2334.
- [3] K. Nishizawa, S.-i. Ishino, H. Watanabe, M. Shinagawa, *J. Nucl. Sci. Technol.* **1984**, *21*, 694–701.
- [4] a) C. W. Hwang, M. H. Jeong, Y. J. Kim, W. K. Son, K. S. Kang, C. S. Lee, T. S. Hwang, *Sep. Purif. Technol.* **2016**, *166*, 34–40; b) L. Ji, Y. Hu, L. Li, D. Shi, J. Li, F. Nie, F. Song, Z. Zeng, W. Sun, Z. Liu, *Hydrometallurgy* **2016**, *162*, 71–78; c) M. J. Park, G. M. Nisola, E. L. Vivas, L. A. Limjoco, C. P. Lawagon, J. G. Seo, H. Kim, H. K. Shon, W.-J. Chung, *J. Membr. Sci.* **2016**, *510*, 141–154; d) R. Trocoli, G. K. Bidhendi, F. La Mantia, *J. Phys. Condens. Matter* **2016**, *28*, 114005.
- [5] a) G. W. Gokel, D. M. Goli, C. Minganti, L. Echegoyen, *J. Am. Chem. Soc.* **1983**, *105*, 6786–6788; b) G. Michaux, J. Reisse, *J. Am. Chem. Soc.* **1982**, *104*, 6895–6899.
- [6] a) B. P. Hay, J. R. Rustad, C. J. Hostetler, *J. Am. Chem. Soc.* **1993**, *115*, 11158–11164; b) J. Guo, J. Lee, C. I. Contescu, N. C. Gallego, S. T. Pantelides, S. J. Pennycook, B. A. Moyer, M. F. Chisholm, *Nat. Commun.* **2014**, *5*, 5389.
- [7] a) R. Krishnakumar, R. S. Swathi, *ACS Appl. Mater. Interfaces* **2016**, *9*, 999–1010; b) M. Kaller, C. Deck, A. Meister, G. Hause, A. Baro, S. Laschat, *Chem. Eur. J.* **2010**, *16*, 6326–6337; c) S. J. Cho, P. A. Kollman, *J. Org. Chem.* **1999**, *64*, 5787–5793; d) R. E. C. Torrejos, G. M. Nisola, H. S. Song, L. A. Limjoco, C. P. Lawagon, K. J. Parohinog, S. Koo, J. W. Han, W.-J. Chung, *Chem. Eng. J.* **2017**, *326*, 921–933.
- [8] H. Staudinger, M. Lüthy, *Helv. Chim. Acta* **1925**, *8*, 65–67.
- [9] I. Hataue, Y. Oishi, M. Kubota, H. Fujimoto, *Tetrahedron* **1991**, *47*, 9317–9328.
- [10] D. J. Cram, *Science* **1988**, *240*, 760–767.
- [11] F. A. L. Anet, in *Dynamic Chemistry*, Springer, **1974**, pp. 169–220.
- [12] L. Calucci, H. Zimmermann, R. Poupko, Z. Luz, *J. Phys. Chem.* **1995**, *99*, 14942–14948.
- [13] S. G. Smith, A. H. Fainberg, S. Winstein, *J. Am. Chem. Soc.* **1961**, *83*, 618–625.
- [14] Y. Shao, L. F. Molnar, Y. Jung, J. Kussmann, C. Ochsenfeld, S. T. Brown, A. T. B. Gilbert, L. V. Slipchenko, S. V. Levchenko, D. P. O'Neill, *Phys. Chem. Chem. Phys.* **2006**, *8*, 3172–3191.
- [15] M. J. Frisch, G. W. Trucks, H. B. Schlegel, G. E. Scuseria, M. A. Robb, J. R. Cheeseman, G. Scalmani, V. Barone, B. Mennucci, G. A. Petersson, *Gaussian Inc. Wallingford CT* **2009**.
- [16] Y. Zhao, D. G. Truhlar, *Theor. Chem. Acc.* **2008**, *120*, 215–241.
- [17] A. V. Marenich, C. J. Cramer, D. G. Truhlar, *J. Phys. Chem. B* **2009**, *113*, 6378–6396.
- [18] a) R. F. Ribeiro, A. V. Marenich, C. J. Cramer, D. G. Truhlar, *J. Phys. Chem. B* **2011**, *115*, 14556–14562; b) I. Funes-Ardoiz, R. S. Paton, (2016). GoodVibes: GoodVibes v1.0.2. <http://doi.org/10.5281/zenodo.595246>.
- [19] T. Bally, P. R. Rablen, *J. Org. Chem.* **2011**, *76*, 4818–4830.
- [20] a) ADF2017.103, SCM Theoretical Chemistry, Vrije Universiteit : Amsterdam (Netherlands), 2017. <http://www.scm.com>; b) C. Fonseca Guerra, J. G. Snijders, G. te Velde, E. J. Baerends, *Theor. Chem. Acc.* **1998**, *99*, 391–403; c) G. te Velde, F. M. Bickelhaupt, E. J. Baerends, C. Fonseca Guerra, S. J. A. van Gisbergen, J. G. Snijders, T. Ziegler, *J. Comput. Chem.* **2001**, *22*, 931–967.
- [21] C. Y. Legault, CYLview, 1.0 b, Université de Sherbrooke, 2009, **2013**.
- [22] J. Dale, T. Ekeland, J. Krane, *J. Am. Chem. Soc.* **1972**, *94*, 1389–1390.
- [23] E. E. Astrup, *Acta Chem. Scand. Ser. A* **1980**, *34*, 85–92.
- [24] M. Kobayashi, S. Kawabata, *Spectrochim. Acta Part A* **1977**, *33*, 549–560.
- [25] Y. Chatani, T. Uchida, H. Tadokoro, K. Hayashi, M. Nishii, S. Okamura, *J. Macromol. Sci. B* **1968**, *2*, 567–590.
- [26] C. Cui, S. J. Cho, K. S. Kim, *J. Phys. Chem. A* **1998**, *102*, 1119–1123.
- [27] It is noteworthy that a previous DFT study on the binding of lithium ion to 6C3 calculated a bending angle of 91.3 degrees for the Li:6C3 complex and gas-phase binding energy for Li<sup>+</sup> of 42 kcal mol<sup>-1</sup>. [ref. 30].
- [28] a) F. M. Bickelhaupt, *J. Comput. Chem.* **1999**, *20*, 114–128; b) F. M. Bickelhaupt, K. N. Houk, *Angew. Chem. Int. Ed.* **2017**, *56*, 10070–10086; *Angew. Chem.* **2017**, *129*, 10204–10221; c) I. Fernández, F. M. Bickelhaupt, *Chem. Soc. Rev.* **2014**, *43*, 4953–4967; d) W.-J. van Zeist, F. M. Bickelhaupt, *Org. Biomol. Chem.* **2010**, *8*, 3118–3127; e) L. P. Wolters, F. M. Bickelhaupt, *WIREs Comput. Mol. Sci.* **2015**, *5*, 324–343.
- [29] a) F. M. Bickelhaupt, A. Diefenbach, S. P. de Visser, L. J. de Koning, N. M. M. Nibbering, *J. Phys. Chem. A* **1998**, *102*, 9549–9553; b) L. Zhao, M. von Hopffgarten, D. M. Andrada, G. Frenking, *WIREs Comput. Mol. Sci.* **2018**, *8*, e1345.
- [30] S. J. Cho, *Bull. Korean Chem. Soc.* **2014**, *35*, 2723–2725.
- [31] N. Alizadeh, *Spectrochim. Acta Part A* **2011**, *78*, 488–493.
- [32] A. J. Smetana, A. I. Popov, *J. Sol. Chem.* **1980**, *9*, 183–196.
- [33] E. Karkhaneei, A. Afkhami, M. Shamsipur, *J. Coord. Chem.* **1996**, *39*, 33–42.
- [34] F. Zaccaria, G. Paragi, C. Fonseca Guerra, *Phys. Chem. Chem. Phys.* **2016**, *18*, 20895–20904.
- [35] F. Cataldo, *Eur. Chem. Bull.* **2015**, *4*, 92–97.
- [36] a) C. Wohlfarth, in *Static Dielectric Constants of Pure Liquids and Binary Liquid Mixtures*, Springer, **2015**, pp. 13–13; b) G. W. Gokel, L. Echegoyen, M. S. Kim, E. M. Eyring, S. Petrucci, *Biophys. Chem.* **1987**, *26*, 225–233.
- [37] E. Raamat, K. Kaupmees, G. Ovsjannikov, A. Trummal, A. Kütt, J. Saame, I. Koppel, I. Kaljurand, L. Lipping, T. Rodima, *J. Phys. Org. Chem.* **2013**, *26*, 162–170.
- [38] R. G. Baum, A. I. Popov, *J. Sol. Chem.* **1975**, *4*, 441–445.
- [39] M. C. Masiker, C. L. Mayne, B. J. Boone, A. M. Orendt, E. M. Eyring, *Mag. Reson. Chem.* **2010**, *48*, 94–100.
- [40] J. B. Lambert, J. E. Goldstein, *J. Am. Chem. Soc.* **1977**, *99*, 5689–5693.
- [41] F. A. Anet, P. J. Degen, *J. Am. Chem. Soc.* **1972**, *94*, 1390–1392.
- [42] N. Sheppard, M. A. Elyashevich, F. A. Miller, E. D. Becker, J. H. Beynon, E. Fluck, A. Hadni, G. Zerbi, G. Herzberg, B. Jeowska-Trzebiatowska, *Pure Appl. Chem.* **1976**, *45*, 217–219.
- [43] D. B. Hibbert, P. Thordarson, *Chem. Commun.* **2016**, *52*, 12792–12805.
- [44] When a 1:2 sandwich complex is assumed, both the extended Roach equation (see Masiker *Magn. Reson. Chem.* **2006**, *44*, 220–229) as well as the corresponding bindfit module yield unrealistic results.

Manuscript received: May 16, 2019  
Revised manuscript received: July 1, 2019  
Accepted manuscript online: July 7, 2019  
Version of record online: July 26, 2019